

Molecular-dynamics simulation of lateral friction in contact-mode atomic force microscopy of alkane films: The role of molecular flexibility

P. SOZA¹, F. Y. HANSEN^{2(a)}, H. TAUB³, M. KIWI^{1,4}, E. CISTERNAS¹, U. G. VOLKMANN¹ and V. DEL CAMPO¹

¹ *Facultad de Física, Pontificia Universidad Católica de Chile - Casilla 306, Santiago, Chile*

² *Department of Chemistry, Technical University of Denmark - IK 207 DTU, DK-2800 Lyngby, Denmark, EU*

³ *Department of Physics and Astronomy and University of Missouri Research Reactor, University of Missouri Columbia, MO 65211, USA*

⁴ *Centro para el Desarrollo de la Nanociencia y la Nanotecnología, CEDENNA - Avda. Ecuador 3493, Santiago, Chile*

received 11 October 2010; accepted in final form 15 June 2011

published online 12 July 2011

PACS 68.37.Ps – Atomic force microscopy (AFM)

PACS 68.35.Af – Atomic scale friction

PACS 31.15.xv – Molecular dynamics and other numerical methods

Abstract – Molecular-dynamics simulations are used to investigate lateral friction in contact-mode atomic force microscopy of tetracosane ($n\text{-C}_{24}\text{H}_{50}$) films. We find larger friction coefficients on the surface of monolayer and bilayer films in which the long axis of the molecules is parallel to the interface than on a surface of molecules with the long axis perpendicular to the surface, in agreement with experimental results. A major dissipation mechanism is the molecular flexibility as manifested in the torsional motion about the molecules' C-C bonds. The generation of *gauche* defects as a result of this motion does not appear to be in itself a major channel of energy dissipation. As previously reported in the literature, the layer density and thereby the strength of the attractive film-tip interaction is also an important factor in energy dissipation.

Copyright © EPLA, 2011

The advent of atomic force microscopy (AFM) has made measurements of the lateral frictional force between a nanoscale object and a molecular film possible [1,2]. This capability allows one to use AFM to correlate friction with film structure and dissipative mechanisms at the molecular level. Friction on the atomic scale has therefore been at the forefront of scientific interest in recent years.

Kreer *et al.* have conducted molecular-dynamics (MD) simulations of the frictional drag between polymer-bearing surfaces [3]. They employ a generic model of polymer chains [4,5] with free rotation about the bonds between monomers and flexible angle bends. Both adsorbed and grafted polymers were considered in good and bad solvents. In all systems, shear thinning is observed and attributed to a stretching of the molecular chains along the sliding direction. For the adsorbed polymers under shear with zero load, they find a proportionality between the friction force and the shear velocity in contrast to the logarithmic dependence found in [6–11].

Mikulski and Harrison (MH) [12] have used MD simulations to examine the tribology associated with the

sliding of a hydrogen-terminated diamond counterface (an infinitely large tip) across a monolayer of n -alkane chains containing 18 carbon atoms (C18) each covalently bonded to a diamond substrate. The long axis of the C18 molecules is tilted slightly from the surface normal and one end of the molecules is covalently bonded to the substrate. The simulations are done with a positive load on the counterface and for two film densities. They conclude that the two most important mechanisms of energy dissipation are vibrational motion of the chain center of mass and bond stretching. These dissipation channels result in a *larger* lateral friction for a system of *lower* density, because chain motion is impeded in the higher-density system despite the stronger tip-film interaction. They also conclude that *gauche*-defect generation seems *not* to be a significant channel of energy dissipation.

Trogisch *et al.* [13] have measured the lateral frictional force in contact-mode AFM measurements on $\text{C}_{32}\text{H}_{66}$ (C32) films deposited on a SiO_2 -coated Si(100) surface. At low coverages, the C32 films show two ordered structures: one or two layers in which the long molecular axis is oriented parallel to the surface (hereafter referred to as parallel layers) followed by partial layers

^(a)E-mail: flemming@kemi.dtu.dk

of perpendicular molecules (hereafter referred to as perpendicular layers) [14–17]. By recording topographic and frictional images simultaneously, they estimated that the lateral frictional force is about 2.5 times smaller on perpendicular layers than on parallel layers. In addition, scans of parallel layers showed different sublevels of friction, which were explained by domains having different azimuthal orientations of the molecules relative to the scan direction.

Here we report MD simulations of the systems studied by Trogisch *et al.* [13], use a comparison between their results and the simulation results to benchmark the simulations, and investigate the dissipative mechanisms responsible for greater lateral friction on the parallel layers. Alkane molecules offer the advantage of relative simplicity without sacrificing the anisotropy and flexibility characteristic of more complex polymers. This simplicity makes it easier both to interpret experimental results and to model them in MD simulations. As will be discussed below, the molecular flexibility introduced in our simulations makes it possible to evaluate the effect of conformational changes on the energy dissipation in the alkane films. In particular, we can monitor the number and distribution of *gauche* defects in the molecules.

To save computation time, we performed simulations on films of the shorter alkane, tetracosane (C24), which forms films having a similar structure as C32; and hence they are expected to exhibit similar frictional properties [18]. We used the united atom model to represent the C24 molecules in which CH_2 and CH_3 groups are replaced by pseudo atoms of the respective mass centered at the C atom positions. Our model includes realistic potentials for angle-bending and dihedral torsional motion, respectively, in order to simulate molecular conformational changes. The simulations are done in the NVT ensemble at room temperature which is ~ 30 K below the C24 bulk melting point, using a Nose-Hoover thermostat. The time step is 2 fs and a predictor-corrector integration scheme of order 5 is used. Periodic boundary conditions are imposed in the x - and y -direction (see fig. 1(a)). Graphite was chosen as the substrate, because we have reliable potentials for the molecule-substrate interaction (see refs. [19] for more details of this model).

Specifically, we treat the friction between an AFM tip and three different systems: i) a parallel monolayer of C24 molecules adsorbed on a graphite substrate; ii) a parallel bilayer of C24 molecules; and iii) a perpendicular monolayer of C24 molecules. Each parallel layer has 64 molecules, while the perpendicular layer has 240 molecules. In practice, we found that molecules in the perpendicular layer actually tilted about 20° from the surface normal, probably because the bulk C24 structure is triclinic rather than orthorhombic [20].

The AFM tip was modeled [21] as a rigid body with atoms arranged to form a truncated pyramid and with the smallest surface closest to the film (see fig. 1). We have considered a tip of 557 atoms with a total mass

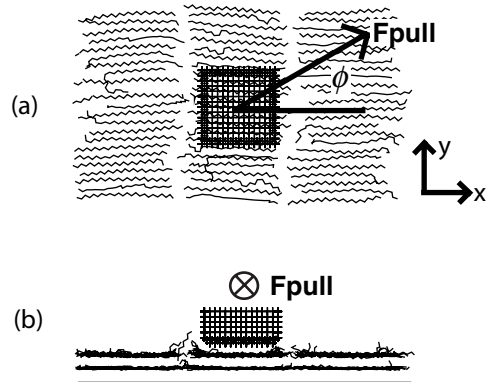


Fig. 1: (a) Definition of the azimuthal angle ϕ between the scan direction and the direction of the long axis of the molecules illustrated by a top-down view of the tip on a parallel bilayer of molecules. (b) A side-view of the tip on a parallel bilayer with a pulling force perpendicular to the direction of the long axis of the molecules ($\phi = 90^\circ$). The simulation box dimensions are $(127.92 \times 76.6) \text{ \AA}^2$ for the parallel layer and $(128.46 \times 38.62) \text{ \AA}^2$ for the perpendicular layer simulations.

$M = 62,384$ amu arranged in 8 layers perpendicular to the z -axis. To save computation time, the tip is “hollow” so that there are only atoms on the tip surfaces with nearest-neighbor atom distance identical to that between pseudo atoms in the alkane molecule. The Lennard-Jones (LJ) interaction potential between tip atoms and the C24 pseudo atoms was chosen to have an ϵ value half that between pseudo atoms to avoid irreproducibility caused by molecules sticking to the tip. He and Robbins [22] have found that a doubling of the interaction (ϵ parameter in the LJ potential) between wall atoms and monomers in an adjacent fluid has almost no effect on the friction. In contrast, the friction increases rapidly with the ratio between the atom-atom distance d in the wall and the σ -parameter in the LJ potential. At the pressures in their studies, the interactions are dominated by the repulsive term in the LJ potential so monomer and wall atoms can be thought of as hard spheres. Therefore, monomers can penetrate deep between wall atoms when the ratio d/σ is large. The effect decreases with decreasing pressure or load and, because our simulations are done at zero load, our results are not expected to depend strongly on the choice of LJ parameters. Moreover, in comparing friction on parallel and perpendicular layers, the effect of the magnitude of the LJ parameters should be eliminated. For the tip atom/graphite C atom interaction, we have used the same (LJ) potential as between a pseudo atom and a graphite C atom. The tip surface nearest to the film consists of a square lattice of atoms with an edge of length of 18.36 \AA , which exceeds several intermolecular distances in the film ($\sim 4\text{--}5 \text{ \AA}$) as does the tip used in the measurements [13]. The atoms in both the tip and the graphite surface are assumed to be static as in other simulations [9,23].

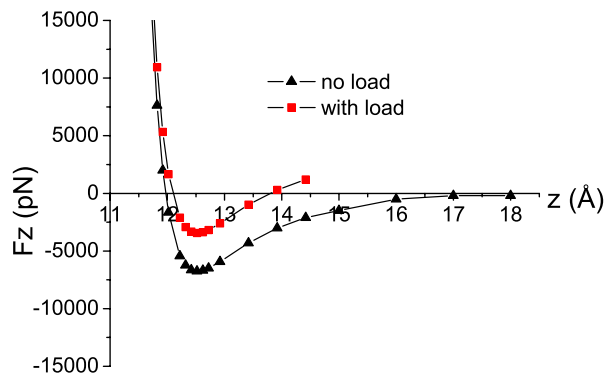


Fig. 2: (Color online) The force between tip and a parallel monolayer of C24 molecules in the z -direction, perpendicular to the layer, as a function of the tip position relative to the solid substrate on which the molecules are adsorbed. Two curves are shown, corresponding to the cases with and without a negative load of 3319 pN applied to the tip. Of the two intersections between the force curve for a negative load and the abscissa axis, each of which represents an equilibrium position, only the one at smaller z is stable.

The system, consisting of the tip and the C24 film below it, was equilibrated for several nanoseconds. We could apply either a zero, a positive, or a negative load to the tip along the surface normal. A negative load may be used to simulate the “near-snap-out” or “attractive” configuration that was used in the measurements [13] to reduce damage to the soft film caused by the tip. However, such a configuration is not quantitatively reproducible in repeated experiments with a given tip. In fig. 2, we have shown the force F_z on the tip with and without a negative load in a direction normal to the surface of a monolayer film. With zero load, the force curve only intersects the abscissa axis at one point, the equilibrium distance of the tip from the molecules, whereas there are two intersections when a negative load is applied. In this case, it is easy to see that only the equilibrium position closest to the C24 molecules is stable. If a fluctuation causes the tip-molecule distance to increase, then the net force along z becomes negative and the tip moves back towards the equilibrium position. If the distance between tip and molecule becomes smaller, then the net force is positive and the tip moves away from the molecules towards the equilibrium position. In contrast, the equilibrium position furthest from the molecules is seen to be unstable by the same analysis. Due to the gradient of the force (and potential) at the stable equilibrium position, the equilibrium distance in the “near-snap-out” configuration only increases by at most 3–4% relative to the zero-load configuration and our simulations have shown a reduction in the friction coefficients of only 10–20%. This insensitivity is fortunate because the load condition is difficult to control quantitatively in measurements in the “near-snap-out” configuration.

After equilibration, we applied a constant lateral pulling force \mathbf{F}_{pull} to the tip to move it across the film. Lateral

forces were applied to the four corner-atoms in the tip, resulting in a net force on the tip equal to \mathbf{F}_{pull} . The other tip-atoms follow the four corner atoms because the tip is rigid. To prevent the tip from rotating and tilting, we added forces to eliminate any torque on the tip so that it only moved laterally across the surface and vertically along the z -direction. As the lateral center-of-mass velocity of the tip increases, the tip-film interaction creates a frictional force opposing the pulling force and, when they balance, the tip moves with a steady velocity.

For the analysis of the results, it is convenient to introduce a friction coefficient f such that the frictional force $\mathbf{F}_{\text{fric}} = -f\mathbf{v}_{\text{cm}}$ is proportional to the center-of-mass velocity of the tip \mathbf{v}_{cm} , when f is constant and independent of the velocity. This condition is met at moderate velocities or equivalently at moderate pulling forces. At higher velocities, the frictional force is found to be nonlinear in the velocity corresponding to a velocity-dependent friction coefficient f . The equation of motion for the tip of mass M may be written as

$$M\dot{\mathbf{V}}_{\text{cm}}(t) = \mathbf{F}_{\text{pull}} - f\mathbf{V}_{\text{cm}}(t), \quad (1)$$

with a steady velocity given by

$$\mathbf{V}_{\text{cm}}^{\text{steady}} = \frac{\mathbf{F}_{\text{pull}}}{M\mu}, \quad (2)$$

where $\mu = f/M$.

For each interface, there exists a range of relevant pulling forces. The upper limit of the pulling force is set by the time-scale of the dissipative processes in the molecular film. When the maximum pulling force is exceeded, the tip slides across the interface with a relatively small frictional force and is unable to attain a steady velocity. For the parallel monolayer and bilayer films of flexible molecules, the maximum pulling force with the given tip was found to be ~ 250 pN compared to ~ 140 pN on the surface of a perpendicular monolayer. The lower limit of the pulling force is set by the magnitude of the friction coefficient and the fluctuations in the system. It was found to be ~ 30 pN and ~ 4 pN for the parallel and perpendicular layers, respectively. Even with the smallest pulling forces in the simulations, we find steady velocities of the order $\sim 2\text{--}50$ ms $^{-1}$, which are still much larger than in the experiments $\sim 2.5 \times 10^{-5}$ ms $^{-1}$. Thus, it is important to conduct simulations for several pulling forces to ensure that we are in the linear region of eq. (2).

In order to specify the scan direction relative to the orientation of the molecules, we have introduced the azimuthal angle ϕ between the scan direction and the direction of the long axis of the molecules, as illustrated by the top-down view of the tip above the parallel bilayer in fig. 1(a).

The results of all simulations are summarized in fig. 3, where we have plotted the steady velocities of the tip $V_{\text{cm}}^{\text{steady}}$ as a function of the pulling acceleration F_{pull}/M . On the perpendicular layer, we have only included the results for one scan direction, $\phi = -69^\circ$ (opposite to the

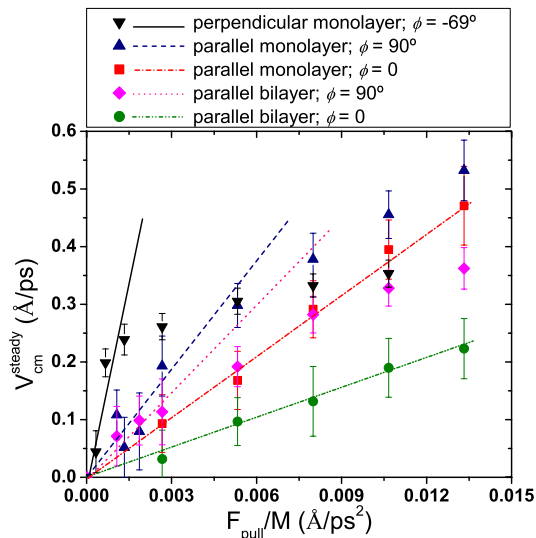


Fig. 3: (Color online) The steady velocity as a function of the pulling acceleration F_{pull}/M for the various systems. Parallel and perpendicular denote a film in which the long axis of the molecules is parallel and perpendicular to the interface, respectively. The slopes of the lines are equal to the reciprocal of $\mu = f/M$ for the various systems. The scan of the perpendicular monolayer at $\phi = -69^\circ$ is in the direction opposite to the molecular tilt (see text).

direction of the molecular tilt from the vertical), because they were practically identical for three different scan directions, just as found in ref. [24] on a system with a perpendicular layer of the shorter $\text{C}_{13}\text{H}_{28}$ alkane. If μ is independent of the pulling force, or equivalently the tip velocity, the data points should lie on a straight line through the origin according to eq. (2). This is seen to be the case for the scans in the direction of the long axis of the molecules ($\phi = 0$) on parallel monolayer and bilayer films. Such a linear relationship was also found in the simulations in ref. [3]. In the other scans, there are obvious departures from a linear dependence of the friction force, which means that μ depends on the pulling force or the velocity. For this reason, we have estimated the slope in the limit $F_{\text{pull}}/M \rightarrow 0$ to compare with experiments. These limiting slopes correspond to scan rates much smaller than in the simulations. The results are compiled in table 1. The nonlinearity at higher velocities is different from the logarithmic relation found in [7,8]. We speculate that this difference may be due to the much higher velocities in our simulations.

For both parallel monolayer and bilayer films, we find a friction coefficient that is a factor of 3 to 11 times larger than for the perpendicular monolayer, depending on the scan azimuth (see table 1). AFM measurements in the contact mode gave a somewhat smaller value for this factor of ~ 2.5 [13]. Because the ϕ angle defined in fig. 1(a) cannot be determined experimentally, this factor represents some azimuthal average. The agreement between the measurements and the simulations is remarkably good, considering that the tip-molecule interaction assumed in the

Table 1: The mass-weighted friction coefficients ($\mu = f/M$) for scanning various films in different directions at zero load. Preliminary simulations of friction with a negative load on a parallel monolayer for scans along the direction of the long molecular axis ($\phi = 0^\circ$) gave $\mu = 24.6 \text{ ns}^{-1}$, a decrease of 10–20%.

System	ϕ	$\mu = f/M$ (ns^{-1})
Parallel monolayer	0°	28.0 ± 0.5
Parallel monolayer	90°	15.9 ± 2.4
Parallel bilayer	0°	58.7 ± 1.4
Parallel bilayer	90°	20.9 ± 1.9
Perpendicular monolayer	-69°	5.2 ± 1.0

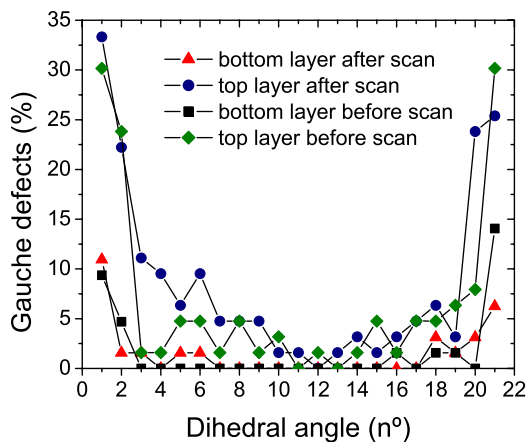


Fig. 4: (Color online) Distribution of *gauche* defects within C_{24} molecules in each layer of a parallel bilayer at 300 K: the average percentage of molecules with *gauche* defects for each of the 21 dihedral bonds before and after a scan with the AFM tip at 300 K. The scan is in the x -direction with a pulling force of 27.6 pN. The bonds are numbered consecutively.

simulations is based solely on the condition that the tip does not damage the film. The results appear to be robust and independent of the details of the interaction potential.

It is of particular interest to investigate the sources of the dissipative processes in the film responsible for the lateral friction force. We have focused on both the flexibility of the alkane molecules and their translational and rotational motions. By flexibility we mean the torsional rotation about the C–C bonds in the alkane chains that may lead to molecular conformational changes as *gauche* defects are introduced. There are three stable conformations about each bond, one *trans* and two *gauche*, as specified by the dihedral angle of rotation. The 21 dihedral angles in the C_{24} molecule are numbered consecutively starting with 1 at one end of the molecule. During the simulations, we monitor the molecular configuration about each of the 21 bonds and determine the average percentage of molecules with *gauche* defects at each of the bonds.

In fig. 4, we show the *gauche* defect distribution within the C_{24} molecules of a parallel bilayer. Before the scan, the *gauche* defects are localized at the ends of the molecules

where there are significantly more defects for molecules in the upper layer. In the central region of the chains, the defect level is only marginally higher for molecules in the upper layer. The effect of the scan on the distribution of defects within molecules in the bottom layer is seen to be very modest, whereas the effect is larger for the top layer molecules. This behavior is also reflected in a change of the average end-to-end distance of the top layer molecules from $\sim 28 \text{ \AA}$ to $\sim 26.5 \text{ \AA}$ before and after scanning the tip, respectively. However, on the whole, the effect of the scan on the number and distribution of *gauche* defects in the molecules of the bilayer is rather limited so that the generation of them does not appear to play a major role in the dissipation process. The same conclusions apply to the monolayer film and the perpendicular film. Thus, we reach a similar conclusion for the C24 parallel and perpendicular films as do MH [12] for their system.

However, the molecular flexibility about the C–C bonds may still be important in the dissipation process even without the generation of *gauche* defects. To test that, we used the same approach as in the study of the melting transition in monolayer alkane films [19]. The molecules were stiffened by increasing the *trans-gauche* transition barrier by a factor of three so that no *gauche* defects were formed during the simulation at room temperature, and the motion in the dihedral torsion angles became strongly restricted. The choice of the factor by which the barrier is increased is inconsequential as long as the increased barrier prevents the formation of *gauche*-defects.

Use of the stiffer molecules resulted in a more erratic motion of the tip as it was pulled across the film. We could reduce this random tip motion by increasing the mass of each tip atom at the expense of a longer time to reach a steady velocity. A 100-fold increase in the tip mass gave a proper balance of these two effects.

Simulations with the more massive tip were done on a parallel bilayer film and a perpendicular film with both flexible and stiffened molecules. We did not repeat simulations of the parallel monolayer, believing it unlikely that the results would differ from those of the bilayer.

Similar to fig. 3, we show in fig. 5 a plot of the steady velocity of the heavier tip as a function of the pulling acceleration with $\phi = 0^\circ$ and 90° on a parallel bilayer film of either flexible or stiff molecules. We see that the slope of the lines through the data points is larger for the film with stiff molecules implying more friction on the film of flexible molecules. As a consistency check, we found for flexible molecules values of $\mu = 0.49 \text{ ns}^{-1}$ ($\phi = 0^\circ$) and 0.24 ns^{-1} ($\phi = 90^\circ$), which are about a factor of 100 smaller as expected for the 100 times heavier tip.

We assume that the friction coefficient μ can be written as a sum of a contribution $\mu_{\text{trans-rot}}$ from energy dissipation in the translational and rotational motion of the molecules and a contribution μ_{dih} from the dissipation in the torsional motion about the C–C bonds, $\mu = \mu_{\text{trans-rot}} + \mu_{\text{dih}}$. For the $\phi = 0^\circ$ pull direction, $\mu = \mu_{\text{trans-rot}} = \mu_{\text{stiff}} = 0.104 \text{ ns}^{-1}$ so that $\mu_{\text{dih}} = 0.386 \text{ ns}^{-1}$. Thus, about 78%

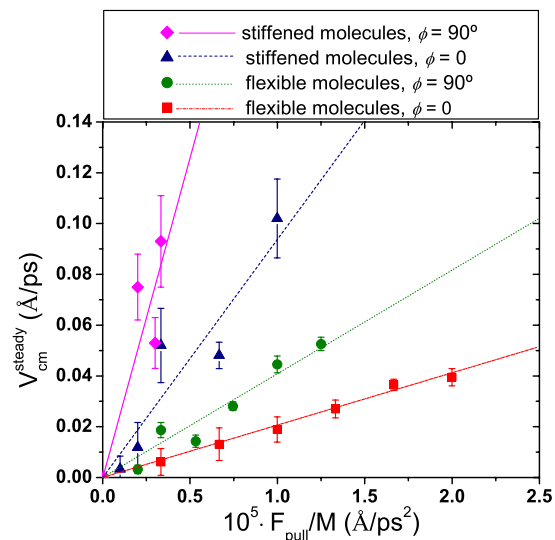


Fig. 5: (Color online) The steady velocity of the heavier tip (100 times the mass of the lighter tip) as a function of the pulling acceleration F_{pull}/M on a parallel bilayer of flexible and stiffened molecules. The slopes of the lines are equal to the reciprocal of $\mu = f/M$ and for $\phi = 0^\circ$ we find, for the system with flexible molecules, $\mu = 0.49 \pm 0.01 \text{ ns}^{-1}$ and, for the system with stiffened molecules, $\mu = 0.10 \pm 0.01 \text{ ns}^{-1}$. For $\phi = 90^\circ$, the system with flexible molecules has $\mu = 0.24 \pm 0.02 \text{ ns}^{-1}$ and the system with stiffened molecules has $\mu = 0.04 \pm 0.007 \text{ ns}^{-1}$.

of the friction in that direction is due to energy dissipation in the dihedral torsion motion. For the $\phi = 90^\circ$ direction, the numbers are $\mu = \mu_{\text{trans-rot}} = 0.0395 \text{ ns}^{-1}$ and $\mu_{\text{dih}} = 0.204 \text{ ns}^{-1}$ so that about 83% percent of the friction in that direction is due to the flexibility of the molecules. These results show that excitation of the torsional modes is a major dissipation mechanism that is nearly independent of the pull-direction. The effect of exciting torsional motion could not be assessed by MH [12], because they only monitored the average energy in the torsion angle without determining the actual number of *gauche* defects and their contribution to the torsional energy. We were unable to determine the friction coefficient in a simulation of a perpendicular layer of stiffened molecules, probably due to its small size.

For both one and two parallel layers, we see from table 1 that μ is smaller in the scan direction perpendicular to the long axis of the molecules ($\phi = 90^\circ$) than parallel to it ($\phi = 0^\circ$). We suggest that the larger friction coefficient is related to the ~ 4 – 5 times higher linear “density” of methylene groups in that direction. Said differently, more C–C contacts are broken in the parallel direction than in the perpendicular direction. A similar argument may be found in ref. [25] for the sliding direction dependence of the friction between two surfaces covered by polytetrafluoroethylene molecules. The dependence of the friction coefficient on the atomic density in the pulling direction is also known from experiments [26,27]. We find from the simulations that the ratio of the μ in the two directions

is ~ 2 and ~ 3 for the monolayer and bilayer, respectively, so that μ does not scale directly with the linear atomic “density”. A possible explanation may be the different ordering of the methylene groups as encountered by the tip in the two azimuthal directions. For $\phi = 0^\circ$, the successive methylene groups interacting with the tip mostly belong to the same molecules, whereas for $\phi = 90^\circ$ they belong to different molecules. The larger μ on a parallel bilayer may be related, as argued in [6], to the larger number of molecules involved in the dissipation process.

We suggest that there are at least two reasons for a smaller friction coefficient on the interface of perpendicular layers than on that of parallel layers. One is the smaller density at the interface of a perpendicular layer. In the simulations, the smaller density results in an attractive tip-film force that is about half that on a parallel layer in agreement with previous rough estimates [28]. A similar density argument was used to explain differences in the frictional force on other films in ref. [6]. Another reason for a smaller friction coefficient on the surface of the perpendicular layer is that only a few dihedral bonds at the end of the molecules can contribute to the energy dissipation process whereas on a parallel layer all dihedral bonds can be involved.

Our explanation of the dependence of the friction coefficient on atomic density contrasts with the findings of MH [12] who found that, for large positive loads, the friction on tightly packed (high-density) monolayers is lower than on loosely packed monolayers. A reason for this discrepancy may be that their molecules have a nearly perpendicular orientation with one end covalently bonded to the substrate. They could be so tightly packed that, when probed with a positive tip load, their motions are impeded and the dissipation thereby reduced. In our case, the molecules have a parallel orientation and are not covalently bonded to the substrate so that under zero load all dihedral bonds can contribute to energy dissipation. Thus, the friction increases in the higher-density parallel bilayer and is larger in the direction of the higher linear density ($\phi = 0^\circ$) as discussed above.

In summary, we have found that the friction coefficient is smaller on the surface of a perpendicular layer than on a parallel layer in agreement with experiment. The simulation results are also consistent with the azimuthal anisotropy of μ inferred indirectly from measurements on a parallel layer. It is caused primarily by a different atomic linear “density” in the scan directions. We find that the flexibility of the molecules as manifested in the torsional motion about the C–C bonds in the alkane chains is the principal source of energy dissipation in the parallel films. However, the torsional motion does not appear to be large enough in amplitude to introduce *gauche* defects in the chains. Both the smaller number of exposed dihedral bonds as well as the smaller atomic density on a perpendicular layer result in it having a lower friction than on a parallel layer. It was also shown that the “near-snap-out” configuration often used

in experiments on soft films is fairly well defined because of the steepness of the tip-film potential in the region around the stable equilibrium. Therefore, the uncertainty in the experimental determination of the friction coefficient is reduced.

This work was supported by Fondo Nacional de Investigaciones Científicas y Tecnológicas (FONDECYT, Chile) under Grants Nos. 1071062, 1090225 (MK), 1060628, 1100882 (UGV) Financiamiento Basal para Centros Científicos y Tecnológicos de Excelencia CEDENNA; by Comisión Nacional de Investigación Científica y Tecnología (CONICYT) (PS); by the U.S. NSF Grant No. DMR-0705974; and by the Danish Center for Scientific Computation, 2800 Lyngby, Denmark.

REFERENCES

- [1] CARPICK R. W. and SALMERON M., *Chem. Rev.*, **97** (1997) 1163.
- [2] PERSSON B.N.J., in *Sliding Friction Physical Principles and Application*, 2nd edition (Springer, Berlin) 2000.
- [3] KREER T. *et al.*, *Langmuir*, **17** (2001) 7804.
- [4] MURAT M. and GREY G. S., *Phys. Rev. Lett.*, **63** (1989) 1074.
- [5] GREY G. S., *Phys. Rev. Lett.*, **76** (1996) 4979.
- [6] BOUHACINA T. *et al.*, *Phys. Rev. B*, **56** (1997) 7694.
- [7] GNECCO E. *et al.*, *Phys. Rev. Lett.*, **84** (2000) 1172.
- [8] STARK R. W. *et al.*, *Ultramicroscopy*, **100** (2004) 309.
- [9] HE G. *et al.*, *Science*, **284** (1999) 1650.
- [10] MARTINI A. *et al.*, *Tribol. Lett.*, **36** (2009) 63.
- [11] BENNEWITZ R. *et al.*, *Phys. Rev. B*, **60** (1999) R11301.
- [12] MIKULSKI P. T. and HARRISON J. A., *J. Am. Chem. Soc.*, **123** (2001) 6873.
- [13] TROGISH S. *et al.*, *J. Chem. Phys.*, **123** (2005) 154703.
- [14] MERKL C. *et al.*, *Phys. Rev. Lett.*, **79** (1997) 4625.
- [15] NOZAKI K. *et al.*, *Jpn. J. Appl. Phys.*, **46** (2007) 761.
- [16] VOLKMAN U. G. *et al.*, *J. Chem. Phys.*, **116** (2002) 2107.
- [17] MO H. *et al.*, *Chem. Phys. Lett.*, **377** (2003) 99.
- [18] BAI M. *et al.*, *EPL*, **79** (2007) 26003.
- [19] HANSEN F. Y. *et al.*, *J. Chem. Phys.*, **98** (1993) 4128; VELASCO E. and PETERS G. H., *J. Chem. Phys.*, **102** (1995) 1098.
- [20] GERSON A. R. and NYBURG S. C., *Acta Crystallogr. B*, **48** (1992) 737.
- [21] SOZA P., PhD dissertation, *Theoretical and experimental studies of the structure and dynamical properties of alkane films*, Pontificia Universidad Católica Santiago de Chile, 2009.
- [22] HE G. and ROBBINS M. O., *Tribol. Lett.*, **10** (2001) 7.
- [23] MÜSER M. H., *Comput. Phys. Commun.*, **146** (2002) 54.
- [24] OHZONO T. and FUJIHIRA M., *Tribol. Lett.*, **9** (2000) 63–67.
- [25] BARRY P. R. *et al.*, *J. Phys.: Condens. Matter*, **21** (2009) 144201; SAWYER W. G. *et al.*, *J. Phys.: Condens. Matter*, **20** (2008) 354012.
- [26] CARPICK R. W. *et al.*, *Tribol. Lett.*, **7** (1999) 79.
- [27] MARCUS M. S. *et al.*, *Phys. Rev. Lett.*, **88** (2002) 226103.
- [28] BAI M. *et al.*, *Ultramicroscopy*, **108** (2008) 946.